Balanced Symmetrical Quasi-Reflectionless Singleand Dual-Band Bandpass Planar Filters

Roberto Gómez-García[®], Senior Member, IEEE, José-María Muñoz-Ferreras[®], Member, IEEE, Wenjie Feng[®], Senior Member, IEEE, and Dimitra Psychogiou[®], Member, IEEE

Abstract - Microwave planar balanced single-/dual-band bandpass filters (BPFs) with symmetrical quasi-reflectionless differential-mode behavior are presented in this letter. They are made up of a direct single-/dual-band BPF branch with virtually short-ended stubs in differential-mode operation, whose input and output accesses are loaded with stub-loaded-type single-/dual-band bandstop filter (BSF) branches that are terminated with a resistor. These BSF branches exhibit a quasicomplementary transfer function with regard to the one of the BPF branch and absorb the differential-mode inputsignal energy not transmitted by the filter to achieve quasireflectionlesss capabilities. The theoretical foundations of the proposed balanced quasi-absorptive single-/dual-band BPFs and synthesis examples are given. Furthermore, for experimentaldemonstration purposes, microstrip prototypes of 3-GHz secondorder single-band and 2.85/3.15-GHz first-order dual-band BPFs are manufactured and characterized.

Index Terms—Absorptive filter, balanced filter, bandpass filter (BPF), bandstop filter (BSF), differential-mode filter, dual-band filter, multiband filter, reflectionless filter, stub-loaded filter.

I. INTRODUCTION

THE development of balanced or differential-mode microwave circuits has acquired a relevant interest in the past few years. When compared to their single-ended counterparts, they offer advantages in terms of higher robustness to undesired noise, crosstalk, and electromagnetic interference phenomena appearing in modern RF systems [1]. On the other hand, high-frequency passive components with reflectionless or absorptive capabilities are also required to protect adjacent active stages from unwanted RF-signal-power reflections that can deteriorate their operation. For example, they can reduce undesired spurious products in mixers that may result from the remixing of these RF-power returns with the local oscillator or minimize instability problems in power amplifiers without the need for additional interstage attenuators [2].

Manuscript received April 6, 2018; revised June 3, 2018; accepted July 10, 2018. Date of publication August 3, 2018; date of current version September 4, 2018. This work was supported in part by the Spanish Ministry of Economy and Competitiveness under Project TEC2017-82398-R, in part by the National Science Foundation under Award 1731956, and in part by the National Natural Science Foundation of China under Grant 6182200033 (Corresponding authors: Roberto Gómez-García; Wenjie Feng.)

R. Gómez-García and J.-M. Muñoz-Ferreras are with the Department of Signal Theory and Communications, University of Alcalá, 28871 Alcalá de Henares, Spain (e-mail: roberto.gomez.garcia@ieee.org; jm.munoz@uah.es).

W. Feng is with the Department of Communication Engineering, Nanjing University of Science and Technology, Nanjing 210094, China (e-mail: fengwenjie1985@163.com).

D. Psychogiou is with the Department of Electrical, Computer, and Energy Engineering, University of Colorado at Boulder, Boulder, CO 80309 USA (e-mail: dimitra.psychogiou@colorado.edu).

Color versions of one or more of the figures in this paper are available online at http://ieeexplore.ieee.org.

Digital Object Identifier 10.1109/LMWC.2018.2856400

A large variety of approaches of balanced planar filtering devices [3]–[6] and reflectionless planar filters [7]–[10] have been reported in the technical literature for different types of transfer function which are either static or reconfigurable. However, no filter solutions that hybridize these two capabilities have been proposed. Although some efforts have been made to realize quasi-absorptive common-mode suppression in balanced filters as in [11], their differential-mode filtering process has a reflective nature with large RF-signal-power levels returned at their terminals in their stopband regions.

In this letter, balanced planar single- and dual-band bandpass filters (BPFs) with symmetrical quasi-reflectionless differential-mode behavior are presented for the first time. They use quasi-absorptive resistively terminated bandstop filter (BSF) branches that are connected to the input-output ports of the filter, which exhibit a nearly complementary transfer function in relation to the one of the differential-mode transmission path. In this manner, the nontransmitted differential-mode input-signal energy in the stopband regions of the overall differential-mode transfer function is routed to the loading resistors of these BSF branches that dissipate it.

The organization of the rest of this letter is as follows: the operational foundations and circuit architectures of the proposed balanced symmetrical quasi-reflectionless filters, along with the theoretical synthesis examples for single-and dual-band BPF realizations, are detailed in Section II. In Section III, the simulated and experimental results of two manufactured proof-of-concept microstrip prototypes of single- and dual-band BPFs are shown. Finally, a summary and the most relevant conclusions of this letter are provided in Section IV.

II. THEORETICAL FOUNDATIONS

The circuit architecture of the engineered balanced symmetrical quasi-reflectionless BPF, upper half for Kth-order realization, is shown in Fig. 1. As can be seen, it is shaped by a direct input-output Kth-order BPF branch with quarterwavelength-at- f_d stubs of Z_R characteristic impedance terminated in a virtual short circuit for differential-mode operation. This BPF branch is loaded at its input-output terminals with resistively terminated Kth-order BSF branches that exhibit a nearly complementary transfer function with regard to that of the BPF branch in differential-mode operation. In this manner, the nontransmitted input-signal energy in the differential-mode stopband regions can be dissipated in the loading resistor of these BSF branches instead of being reflected back at the filter accesses. Hence, a differential-mode quasi-reflectionless behavior is obtained in this stub-loaded balanced filter. For common-mode operation, the stubs of the direct input-output path are terminated in a virtual open circuit, so that a reflectivetype BSF nature is attained in the overall filter to inhibit

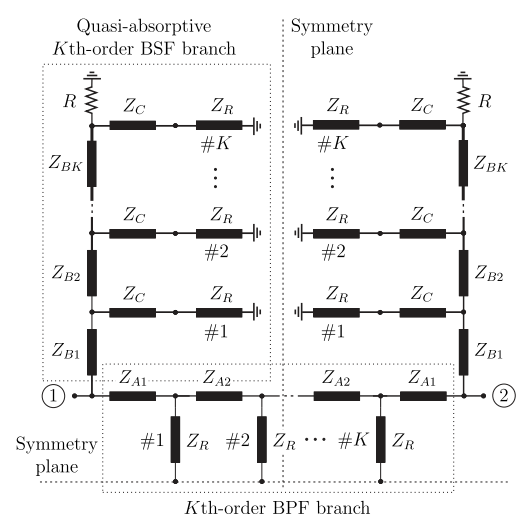


Fig. 1. Circuit detail—upper half—of the proposed Kth-order symmetrical quasi-reflectionless single-band BPF (Z_R -characteristic-impedance transmission-line segments are resonators and the rest are impedance inverters; all these lines have an electrical length of 90° at the design frequency f_d).

common-mode transmission. In relation to the theoretical design of the proposed symmetrical quasi-reflectionless BPF topology, which is frequency periodic with the first spectral period being $[0, 2f_d)$, the following considerations must be taken into account.

- 1) For first-order designs, i.e., K=1, and frequency-independent impedance inverters, it can be verified by following a similar procedure as in [9] that the relationship $Z_C=Z_{A1}Z_{B1}/Z_0$ results in a minimum differential-mode power matching level of 15.15 dB across the entire frequency range. However, for transmission-line-based inverters as in Fig. 1, a fine tuning of Z_C around this value may be needed for the adjustment of the power matching performance within the entire differential-mode transmission band at the filter accesses. An optimization process is also necessary in higher order realizations, for which the derivation of analytical synthesis equations becomes more complicated as the filter order increases.
- 2) The line impedance parameter Z_R , among some other design variables as degrees of freedom depending on the filter order, allows to control the differential-mode passband width while preserving the quasi-reflectionless and in-band common-mode rejection filter capabilities.

For illustration purposes of the previous remarks, Fig. 2 depicts the differential-mode power transmission, reflection, and common-mode power-rejection responses of theoretically synthesized first- and second-order examples of the balanced quasi-reflectionless BPF in Fig. 1 for a 3-dB absolute bandwidth of $0.235\,f_d$. Specifically, a 13.8-dB differential-mode power-matching bandwidth of $0.92\,f_d$ centered at f_d , i.e., 3.8 times the 3-dB passband width, is obtained in both cases, with higher differential-mode selectivity and common-mode rejection as the filter order increases. On the other hand, for the second-order example in Fig. 2, Fig. 3 reveals how a higher Z_R value results in a broader differential-mode transmission band.

Finally, the extension of the engineered balanced quasireflectionless single-band BPF concept to dual-band BPF realizations is verified in Fig. 4. In particular, the circuit detail of the first-order dual-band BPF and BSF branches to be used in the scheme of Fig. 1 for that purpose and two theoretically

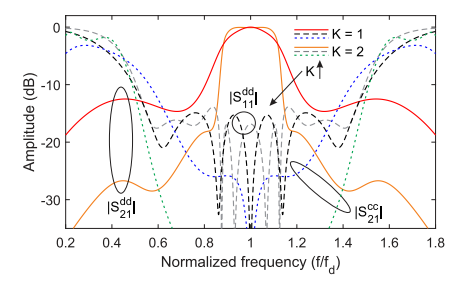


Fig. 2. Theoretical differential-mode power transmission ($|S_{21}^{\rm dd}|$), reflection ($|S_{11}^{\rm dd}|$), and common-mode power transmission ($|S_{21}^{\rm cc}|$) responses of ideally synthesized first- and second-order examples for the balanced quasi-reflectionless single-band BPF in Fig. 1: order variation ($K=1:Z_{A1}=1.16Z_0,\ Z_{B1}=Z_0,\ Z_C=Z_0,\ Z_R=0.46Z_0,\ {\rm and}\ R=Z_0;\ K=2:Z_{A1}=1.5Z_0,\ Z_{A2}=2.6Z_0,\ Z_{B1}=1.1Z_0,\ Z_{B2}=Z_0,\ Z_C=Z_0,\ Z_R=0.5Z_0,\ {\rm and}\ R=Z_0;\ Z_0 \ {\rm is}\ {\rm the\ reference\ impedance}).$

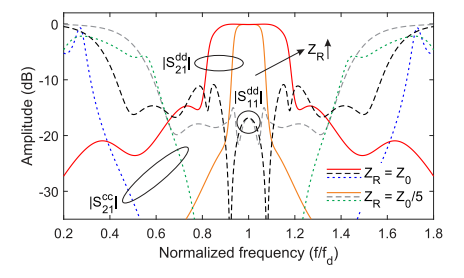


Fig. 3. Theoretical differential-mode power transmission ($|S_{21}^{\rm dd}|$), reflection ($|S_{11}^{\rm dd}|$), and common-mode power transmission ($|S_{21}^{\rm cc}|$) responses of ideally synthesized second-order examples for the balanced quasi-reflectionless single-band BPF in Fig. 1: bandwidth variation through Z_R (the rest of the design parameter values are the same as in the second-order example in Fig. 2).

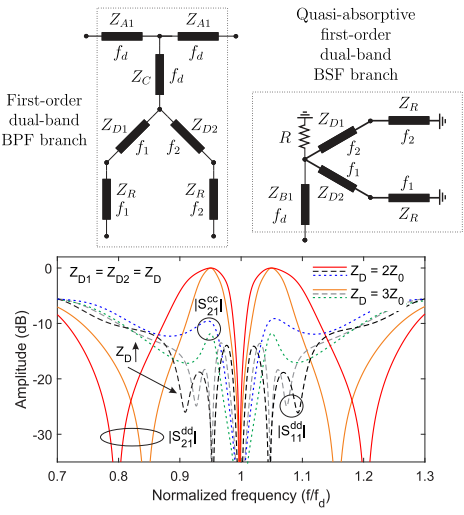


Fig. 4. Dual-band BPF and BSF branches for first-order realizations of balanced quasi-reflectionless dual-band BPFs $(f_1 \text{ and } f_2)$: center frequencies of the lower and upper passbands; $f_d = (f_1 + f_2)/2$; and the electrical lengths of all the transmission-line segments are equal to 90° at the indicated frequencies) and theoretical differential-mode power transmission $(|S_{21}^{\text{cd}}|)$, reflection $(|S_{11}^{\text{cd}}|)$, and common-mode power transmission $(|S_{21}^{\text{cc}}|)$ responses of associated ideally synthesized dual-band BPF examples $(f_1 = 0.85 f_d, f_2 = 1.15 f_d, Z_{A1} = Z_0, Z_{B1} = Z_0, Z_C = Z_0, Z_R = 0.46 Z_0, \text{ and } R = Z_0)$.

synthesized examples with lower and upper band center frequencies of $f_1 = 0.85 f_d$ and $f_2 = 1.15 f_d$ are shown. Also, note that different bandwidths for the dual passbands can be set by making $Z_{D1} \neq Z_{D2}$. Moreover, like in the single-band BPF case, higher order and in-series cascade dual-band BPF realizations are feasible to increase the out-of-band differential-mode and in-band common-mode suppression levels.

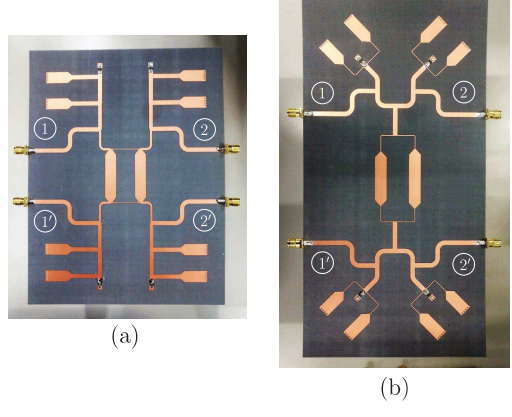


Fig. 5. Photographs of the manufactured balanced quasi-reflectionless microstrip filter prototypes (Rogers 5880 substrate: relative dielectric permittivity $\varepsilon_r = 2.2$, dielectric thickness H = 1 mm, metal thickness $t = 35~\mu$ m, and dielectric loss tangent $\tan(\delta_D) = 0.0009$; ground connections for 50- Ω resistors: 1-mm-diameter metallic via holes). (a) Single-band BPF (core area: $16.9 \times 11.5~\text{cm}^2$). (b) Dual-band BPF (core area: $21.4 \times 10.1~\text{cm}^2$).

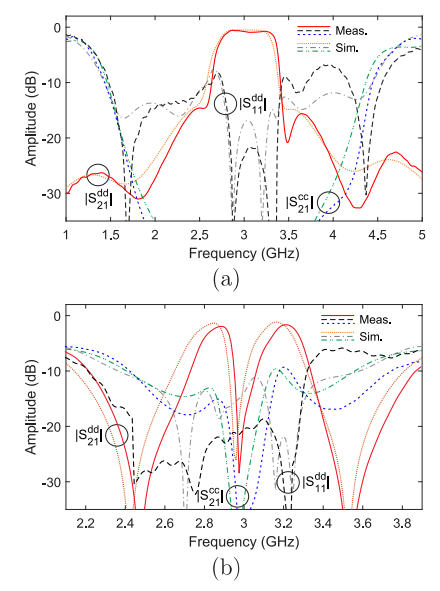


Fig. 6. Simulated and measured differential-mode power transmission ($|S_{21}^{\rm cd}|$), reflection ($|S_{21}^{\rm cd}|$), and common-mode power transmission ($|S_{21}^{\rm cc}|$) responses of the manufactured balanced quasi-reflectionless microstrip filter prototypes. (a) Single-band BPF. (b) Dual-band BPF.

III. EXPERIMENTAL RESULTS

To verify the practical usefulness of the described balanced quasi-reflectionless single- and dual-band BPF principles, two microstrip prototypes have been built and tested. They, respectively, correspond to the second-order single-band and first-order dual-band BPFs synthesized in Fig. 2—case K=2—and Fig. 4— $Z_{D1}=Z_{D2}=5Z_0/2$ and the other design variables as in the examples there—for $f_d=3$ GHz and $Z_0=50$ Ω .

The photographs of the manufactured microstrip prototypes are shown in Fig. 5. Its simulated—by means of the commercial package Ansys HFSS—and measured—with an Agilent-E8361A network analyzer—differential-mode power transmission, reflection, and common-mode power transmission parameters are depicted in Fig. 6. As can be seen, a reasonable agreement between simulations and measurements is obtained that experimentally demonstrates the quasireflectionless behavior. Some discrepancies are observed in terms of a decrease of the input power matching levels in the

upper stopband range of both prototypes that are attributed to manufacturing and loading resistor tolerances. For the singleband BPF circuit, the main measured characteristics are as follows: differential-mode operation with center frequency of 3.04 GHz, 3-dB absolute bandwidth of 662 MHz (i.e., equal to 21.8% in relative terms), minimum in-band power insertion loss level of 0.6 dB, minimum in-band power matching level of 8.3 dB, and common-mode power-rejection levels higher than 35 dB within the differential-mode passband. The dual-band BPF exhibits differential-mode lower and upper passbands with center frequencies of 2.82 and 3.21 GHz, 3-dB absolute bandwidths of 150 and 165 MHz (i.e., equal to 5.2% and 5.1% in relative terms), minimum in-band power-insertion-loss levels of 1.9 and 1.7 dB, and minimum in-band power matching levels of 21.6 and 16.1 dB. The minimum common-mode power-rejection levels within the lower and upper differential-mode 3-dB passband widths are 15.1 and 9.3 dB, respectively.

IV. CONCLUSION

A class of single-/dual-band microwave planar BPFs with symmetrical quasi-reflectionless capabilities in differential-mode operation has been proposed for the first time. It has been shown that the order increase in these filters results in higher differential-mode selectivity and in enhanced in-band common-mode suppression while keeping the quasi-absorptive behavior. Guidelines for the design and bandwidth adjustment of the devised balanced quasi-reflectionless filters, which are scalable to more than two-passband schemes, have been given. Moreover, two proof-of-concept microstrip prototypes consisting of 3-GHz second-order single-band and 2.85/3.15 GHz first-order dual-band BPFs have been developed and tested.

REFERENCES

- [1] F. Martin, L. Zhu, J.-S. Hong, and F. Medina, *Balanced Microwave Filters*, 1st ed. New York, NY, USA: Wiley, 2018.
- [2] Mini-Circuits, Brooklyn, N.Y., "Reflectionless filters improve linearity and dynamic range," *Microw. J.*, vol. 58, no. 8, pp. 42–50, Aug. 2015.
- [3] W. Feng, W. Che, and Q. Xue, "The proper balance: Overview of microstrip wideband balance circuits with wideband common mode suppression," *IEEE Microw. Mag.*, vol. 16, no. 5, pp. 55–68, Jun. 2015.
- [4] S.-X. Zhang, Z.-H. Chen, and Q.-X. Chu, "Compact tunable balanced bandpass filter with novel multi-mode resonator," *IEEE Microw. Wireless Compon. Lett.*, vol. 27, no. 1, pp. 43–45, Jan. 2017.
- [5] A. Fernández-Prieto, A. Lujambio, F. Martín, J. Martel, F. Medina, and R. R. Boix, "Compact balanced-to-balanced diplexer based on split-ring resonators balanced bandpass filters," *IEEE Microw. Wireless Compon. Lett.*, vol. 28, no. 3, pp. 218–220, Mar. 2018.
- [6] R. Gómez-García, R. Loeches-Sánchez, D. Psychogiou, and D. Peroulis, "Multi-stub-loaded differential-mode planar multiband bandpass filters," *IEEE Trans. Circuits Syst. II, Exp. Briefs*, vol. 65, no. 3, pp. 271–275, Mar. 2018.
- [7] A. C. Guyette, I. C. Hunter, and R. D. Pollard, "Design of absorptive microwave filters using allpass networks in a parallel-cascade configuration," in *IEEE MTT-S Int. Microw. Symp. Dig.*, Boston, MA, USA, Jun. 2009, pp. 733–736.
- [8] M. A. Morgan and T. A. Boyd, "Theoretical and experimental study of a new class of reflectionless filter," *IEEE Trans. Microw. Theory Techn.*, vol. 59, no. 5, pp. 1214–1221, May 2011.
- [9] D. Psychogiou and R. Gómez-García, "Reflectionless adaptive RF filters: Bandpass, bandstop, and cascade designs," *IEEE Trans. Microw. Theory Techn.*, vol. 65, no. 11, pp. 4593–4605, Nov. 2017.
- [10] R. Gómez-García, J.-M. Muñoz-Ferreras, and D. Psychogiou, "Symmetrical quasi-reflectionless BSFs," *IEEE Microw. Wireless Compon. Lett.*, vol. 28, no. 4, pp. 302–304, Apr. 2018.
- [11] C.-Y. Hsiao, C.-H. Cheng, and T.-L. Wu, "A new broadband common-mode noise absorption circuit for high-speed differential digital systems," *IEEE Trans. Microw. Theory Techn.*, vol. 63, no. 6, pp. 1894–1901, Jun. 2015.